J Mater Sci (2007) 42:9795–9800
DOI 10.1007/s10853-007-1992-0

Effects of oxygen pressure on the structure and photoluminescence of ZnO thin films

Changzheng Wang · Dongran Xu · Xiaoguang Xiao · Yiqing Zhang · Dong Zhang

Received: 13 December 2006 / Accepted: 12 July 2007 / Published online: 18 August 2007
© Springer Science+Business Media, LLC 2007

Abstract A series of ZnO thin films were deposited on silicon (100) substrate at 473 K by using facing target RF magnetron sputtering system at different oxygen pressure in this paper. The structure, surface morphology and photoluminescence of the ZnO thin films were characterized by X-ray diffraction, atomic force microscopy (AFM), and photoluminescence spectra (PL), respectively. The results showed that only a (002) peak of hexagonal wurtzite appeared in all ZnO thin films, indicating that ZnO films exhibited strong texture. With increasing the oxygen pressure, the results indicated that the ZnO film deposited at 1.2 Pa Ar pressure and 0.6 Pa oxygen pressure had the best preferential *C*-axis orientation and the weakest compressive stress. Meanwhile, AFM observation showed that ZnO film deposited at pure Ar had the highest surface roughness. With the increment of oxygen pressure, the surface roughness decreased gradually. In addition, PL measurement showed that the ZnO film deposited at 1.2 Pa Ar pressure and 0.6 Pa oxygen pressure had the strongest ultraviolet emission and the weakest blue emission.

Introduction

So far Zinc oxide (ZnO) thin films have been investigated extensively because of their many remarkable characteristics such as electrical, optical and piezoelectric properties making suitable for many applications including transparent conductive films, solar cell window and MEMS wave devices [1, 2]. Many techniques, including metal organic chemical vapor deposition [3], laser molecular beam epitaxy [4], pulsed laser deposition [5], sol–gel [6], and radio frequency (RF) magnetron sputtering [7–10], were used to fabricate ZnO thin films on a variety of substrates, such as sapphire, glass, and silicon etc. Especially, the RF magnetron sputtering is widely employed to fabricate ZnO thin films due to its advantages of easy control for the preferred crystalline orientation, growing at relatively low temperature, good interfacial adhesion to the substrate and the high packing density of the grown film. However, in conventional RF magnetron sputtering system, the target and the substrate are set facing, thus resulting in worse uniformity etching of target and lower utilization of target. Moreover, the bombardment to ZnO thin film is aggrandized by high-energy particles. In order to avoid these problems, in this paper we use the facing target RF magnetron sputtering system to deposit ZnO films on the silicon substrate since silicon is not only of interest for the integration of optoelectronic devices but also cheaper and easier to cleave in comparison to other substrates. On the other hand, since some oxygen vacancies usually occur in ZnO films after sputtering, we combined Ar gas with oxygen gas to deposit ZnO films in order to make up for the shortage of oxygen in ZnO films and prepared a series of ZnO films at various oxygen pressure. Meanwhile, we also studied the effects of oxygen pressure on the structure, surface morphology and photoluminescence of ZnO films in detail.

C. Wang (✉) · D. Xu · X. Xiao · Y. Zhang · D. Zhang
School of Physics Science and Information Engineering, Liaocheng University, Liaocheng 252059 Shandong Province, P.R. China
e-mail: wangchangzheng@lcu.edu.cn

Experimental details

A facing target RF magnetron sputtering system, which was illustrated in Fig. 1 [11], was used to deposit ZnO thin

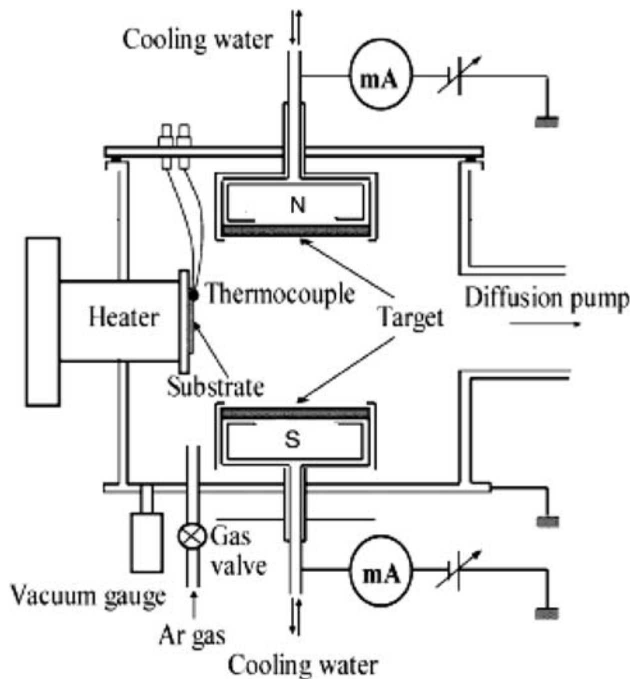

Fig. 1 Schematic diagram of the facing target RF magnetron sputtering system

films on Si (100) substrate. As can be seen from Fig. 1, two sintered ceramic ZnO targets (99.99%) with diameter of 4 cm were set facing and their distance is about 8 cm. The direction of homogeneous magnetic field is from top target to below target. Before sputtering, the silicon substrate was supersonically cleaned in acetone, alcohol for half an hour in sequence to remove grease and organic contaminations. Then, in order to remove silicon oxide on the silicon surface, the substrate was treated with 5% HF solution, washed with deionized water and blown off by pure nitrogen before set into the vacuum chamber. The sputtering was performed by supplying RF power of 200 W with a frequency of 13.56 MHz after the sputtering chamber was evacuated to a base pressure of 4.5×10^{-4} Pa. The mixed atmosphere of Ar (99.999%) and oxygen (99.999%) was introduced into sputtering chamber and their partial pressures were regulated by two mass flow controllers, respectively. The Ar pressure was set constant as 1.2 Pa and the oxygen pressure was chosen as 0, 0.6, 1.2, 1.8, and 2.4 Pa, respectively. The substrate was heated to about 473 K and the sputtering time was 3 h. In order to clean the targets surface, the pre-sputtering was performed about 30 min.

The structure of ZnO thin films was measured by using X-ray diffractometer (XRD, Bruker D8 Advance) with Cu-Ka radiation ($\lambda = 0.15406$ nm) and the surface morphology of ZnO thin films was characterized by using atomic force microscope (AFM, AJ-IIIa). The photoluminescence (PL) spectra were measured with excitation wavelength 325 nm by using Edinburgh Instruments FLS920 type spectrofluorophotometer and photo multiplier tube (PMT) detector, and the exciting light source was Xe-lamp with 450 W. A cutoff filter to puss only waves above 345 nm was used to block the lights scattered from the source. All experiments were carried on at room temperature.

Results and discussion

Structure and surface morphology

Figure 2 shows XRD spectra of ZnO thin films deposited at different oxygen pressure. It is apparent that only a (002) peak of hexagonal wurtzite appears in all ZnO thin films, indicating that all ZnO films exhibit (002) preferential orientation with the *C*-axis perpendicular to the substrate surface and have strong texture. With the increment of the oxygen pressure, the (002) peak intensity first increases and then decreases gradually, reaching a maximum at 0.6 Pa oxygen pressure, which is also shown in Fig. 3. Meanwhile, it is clear that the full width at half maximum (FWHM) of ZnO (002) peak first decreases and then increases with increasing the oxygen pressure, reaching a minimum at 0.6 Pa oxygen pressure, which is similar to the experimental results by DC reactive magnetron sputtering the metallic Zn [12]. These phenomena can be explained as follows. For ZnO thin film deposited at pure Ar, there exists lots of oxygen vacancies, thus resulting in the fact that the chemical composition of ZnO film is non-stoichiometric

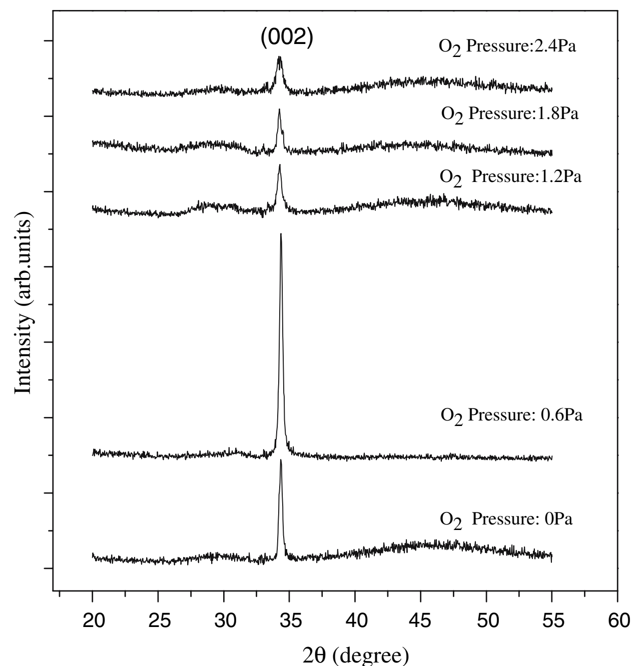

Fig. 2 XRD spectra of ZnO thin films deposited at different oxygen pressure

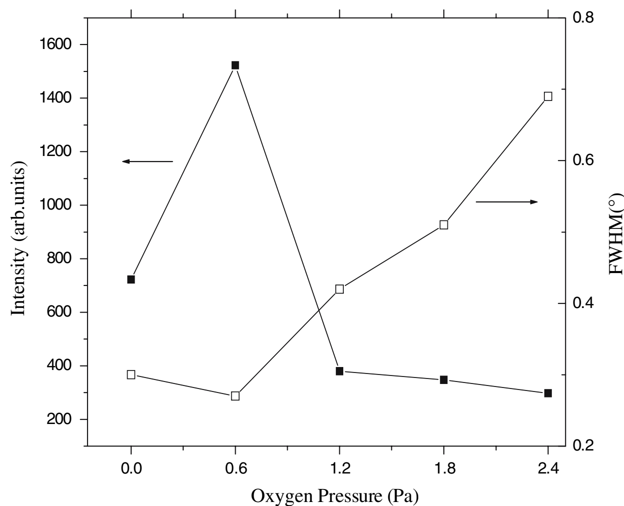

Fig. 3 The intensity (■) and FWHM (□) of (002) peak for ZnO thin films deposited at different oxygen pressure

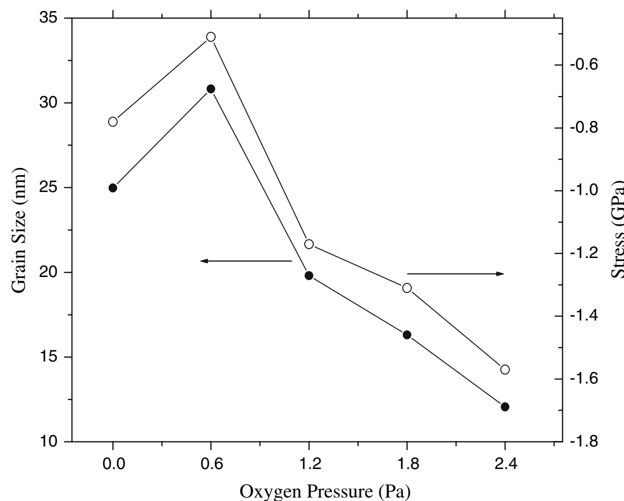

Fig. 4 Grain size (•) and stress (○) of ZnO thin films deposited at different oxygen pressure

and then the ZnO thin film has worse crystalline. Therefore, ZnO thin film deposited at pure Ar has low (002) peak intensity and large FWHM. With increasing the oxygen pressure of about 0.6 Pa, the stoichiometry between Zn and O is improved and then ZnO thin film has better crystalline, thus resulting in higher (002) peak intensity and lower FWHM. While with increasing the oxygen pressure further, the stoichiometry between Zn and O in ZnO thin films is worsen by introducing interstitial oxygen atoms into ZnO thin films and then ZnO thin films have worse crystalline, thus resulting in the decrease of ZnO (002) peak intensity and the increment of the FWHM of ZnO (002) peak. Therefore, we draw a conclusion that the ZnO thin film deposited at 1.2 Pa Ar pressure and 0.6 Pa oxygen pressure has the best preferential *C*-axis orientation.

As well known that the grain size play a key role in the structure and properties of ZnO film, therefore, it is indispensable to study the grain size in the ZnO films. According to Scherrer formula, the grain size can be estimated as follows [13]:

$$D = \frac{0.9\lambda}{B\cos\theta} \tag{1}$$

where D, λ, B, and θ are the grain size, the X-ray wavelength, the FWHM, and Bragg diffraction angle, respectively. The calculated results are shown in Fig. 4. From Fig. 4 one can see that the grain size is about 15–35 nm and reaches a maximum at 0.6 Pa oxygen pressure due to the fact that ZnO films deposited at 0.6 Pa oxygen pressure have best preferential *C*-axis orientation and smallest FWHM, indicating that there exists an optimum oxygen pressure to prepare ZnO thin films with stronger (002) texture.

Besides the grain size, the residual stress also affects the structure and properties of ZnO film significantly. Since there exists a strong (002) texture in ZnO thin film, it is impossible to measure the residual stress by using some method required to measure diffraction peak with different sample orientations, such as Psi-method. Thus we investigate the residual stress in ZnO thin films by analyzing the displacement of (002) peak in XRD spectrum. In the ZnO thin film, the residual stress in the direction parallel to the surface acts as a *C*-axis stress, which is an intrinsic stress originating from the difference of the film structure and density from substrate because the film grew at 473 K [7]. Compared with the standard XRD spectrum of ZnO powder, we found that all the films in our experiment exhibit discrepancy in c-value (c is lattice constant), which is due to the variation of residual stress in the films. To obtain the residual stress σ_{film} in ZnO film, the following formula is used [12]:

$$\sigma_{\text{film}} = \frac{2c_{13}^2 - c_{33}(c_{11} + c_{12})}{2c_{13}} \times \frac{c_{\text{film}} - c_0}{c_0} \tag{2}$$

where c_0 is the lattice constant of standard ZnO powder (c_0 = 0.52054 nm) and c_{film} is the lattice constant of ZnO films deposited in our experiments and can be calculated using following formula:

$$2d\sin\theta = \lambda, \quad c_{\text{film}} = 2d \tag{3}$$

Meanwhile, c_{11}, c_{12}, c_{13}, c_{33} stand for the elastic constants of ZnO film in different directions and are equal to 208.8, 119.7, 104.2, 213.8 GPa, respectively [14]. Substituting c_{11}, c_{12}, c_{13}, and c_{33} value into Eq. 2, we can derive the following formula:

$$\sigma_{\text{film}} = -233 \times \frac{c_{\text{film}} - c_0}{c_0}. \tag{4}$$

According to Eq. 4, we calculated the residual stress of ZnO thin films, as shown in Fig. 4. It can be found that for

ZnO thin film deposited at pure Ar the residual stress behaves as compressive stress, which is in agreement with the results reported by Ondo-Ndong et al. [8]. With increasing the oxygen pressure from 0 to 2.4 Pa, the residual stress keep compressive stress for all ZnO thin films. Meanwhile, the residual compressive stress first decreases and then increases, reaching a minimum value at 0.6 Pa oxygen pressure. This may be attributed to the fact that when the oxygen pressure is about 0.6 Pa, ZnO film has best stoichiometry between Zn atoms and O atoms, thus relaxing the compressive stress of ZnO film. With increasing oxygen pressure gradually, lots of oxygen atoms stay at crystal boundary, resulting in the contraction of ZnO film and then the enhancement of the compressive stress in ZnO film [15].

On the other hand, surface morphology also plays a key role in photoluminescence of ZnO films, therefore, it is important to determine surface morphology of ZnO film by using atomic force microscopy (AFM). The results are shown in Fig. 5. As can be seen from Fig. 5(a) that the ZnO thin film deposited at pure Ar has an irregular pillar structure and larger surface roughness about 7 nm. With increasing the oxygen pressure of 0.6 Pa, the ZnO thin film form the compact, dense uniform island structure and the surface roughness decreases to about 5 nm. With increasing the oxygen pressure further, the surface roughness decreases gradually while the ZnO thin films form an irregular pillar structure that is disadvantageous to the properties of ZnO films. All these observations indicate that ZnO film deposited at 1.2 Pa Ar pressure and 0.6 Pa oxygen pressure has high quality, which is coincided with the XRD analysis in Fig. 2.

Photoluminescence spectra

As mentioned above, structure and surface morphology of ZnO films are essential factors affecting the properties of ZnO film and have been studied in detail. However in the final analysis our main aim is to study and use the PL spectra of ZnO film. Therefore, it is important to disclose the PL spectra of ZnO thin films and the relationship between PL spectra and structure of ZnO films. The PL spectra of ZnO films are measured by using Edinburgh Instruments FLS920 type spectrofluorophotometer and photo multiplier tube (PMT) detector, as shown in Fig. 6. Figure 6 shows the PL spectra of ZnO thin films deposited at various oxygen pressures. It is apparent that all the PL spectra have a UV emission situated at about 375 nm and a blue emission situated at about 470 nm in the visible region, which is similar to the experimental result obtained from the ZnO thin films deposited on Si (111) at different substrate temperature [5]. Meanwhile, with increasing the oxygen pressure the intensity of the UV peak first increases and then decreases, reaching a maximum at 0.6 Pa oxygen pressure. However, the intensity of the blue peak reaches a minimum at 0.6 Pa oxygen pressure and then increases with the increment of oxygen pressure. All these phenomena can be analyzed as follows.

In ZnO film, there exist several kinds of PL spectra including UV emission, violet emission, blue emission, green emission, and so on. They have different emitting mechanisms, among them UV emission in ZnO film is considered as the recombination of free exciton by some papers [9, 16]. It is worthy to notice that the binding energy of the free exciton in ZnO film is about 60 meV under

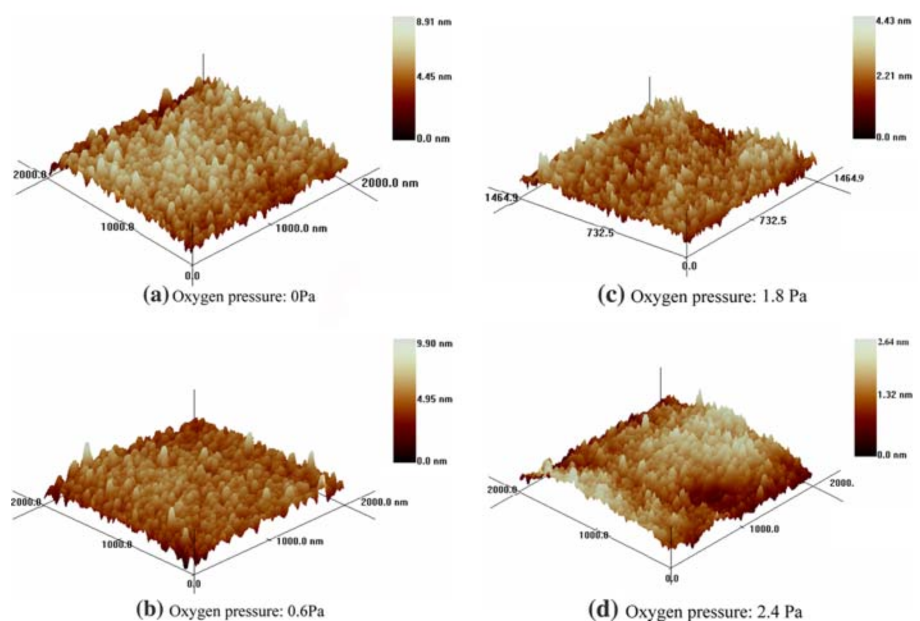

Fig. 5 AFM of ZnO thin films deposited with different oxygen pressure: (**a**) 0 Pa oxygen pressure, (**b**) 0.6 Pa oxygen pressure, (**c**) 1.8 Pa oxygen pressure, (**d**) 2.4 Pa oxygen pressure

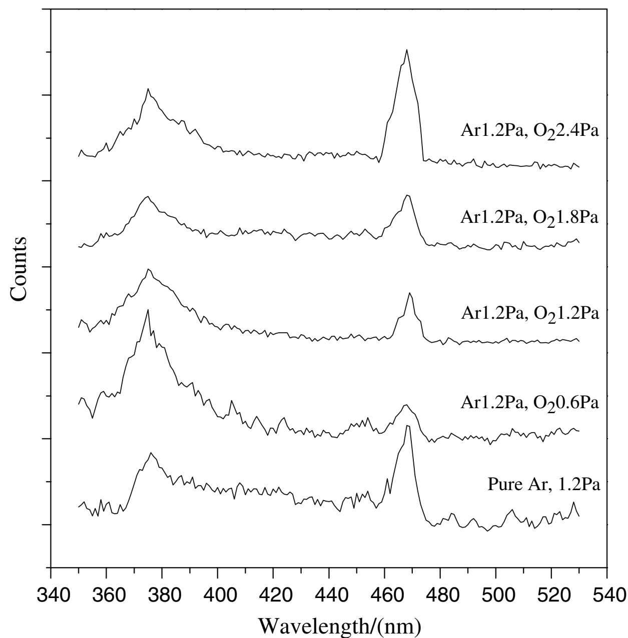

Fig. 6 PL spectra of ZnO thin films deposited at different oxygen pressure

room temperature and is larger than the energy of the free electron skipping from valence band to conduction band, thus resulting in the fact that the probability of free exciton recombination emission is larger than that of band–band transition, and then its emission intensity is much stronger, too. Since the concentration of the free exciton is affected by the crystal quality of ZnO thin films, it will decrease if there are many defects in ZnO thin film. It is well known that there are various defects in ZnO thin films, such as oxygen vacancy, zinc vacancy, interstitial oxygen, interstitial zinc, antisite oxygen, etc. For the ZnO thin film deposited at pure Ar by RF magnetron sputtering method, the chemical composition was non-stoichiometric, and ZnO film usually consists of much oxygen vacancies which are the dominant defect. Therefore, the concentration of the free exciton is small and then the UV peak is weak in the ZnO thin film. With increasing the oxygen pressure to 0.6 Pa, the defect concentration is lower and the concentration of the free exciton is larger, resulting in the enhancement in the intensity of UV peak, as seen in Fig. 6. While with further increasing oxygen pressure, lots of interstitial oxygen occurred in ZnO films, which decrease the crystal quality of ZnO thin films (Fig. 2) and then give rise to lower concentration of the free exciton and lower intensity of UV peak.

On the other hand, oxygen vacancies in ZnO thin films can produce two defect donor levels and the shallower donor level locates below the conduction band about 0.3–0.5 eV [10]. While interstitial oxygen can produce the shallow acceptor level located above the valence band about 0.4 eV [17]. Since the band gap of ZnO is 3.37 eV under room temperature and the energy interval from the shallow donor level to the shallow acceptor level is about 2.6 eV being consistent with the photon energy of the blue emission observed in our study, we believe that the blue emission peak at 468 nm in PL spectra of ZnO film can be attributed to the electron transition between the oxygen vacancies and interstitial oxygen [18]. For ZnO thin film deposited at pure Ar, the blue peak intensity is stronger because of lots of oxygen vacancies in the ZnO. And with the oxygen pressure increasing to 0.6 Pa the blue peak turns weaker because stoichiometric of ZnO film is better and ZnO film has lower oxygen vacancies and interstitial oxygen. However, for ZnO film deposited at higher oxygen pressure the blue peak intensity gets stronger again for much interstitial oxygen occurred in the deposited film.

Conclusions

In summary, we have deposited a series of ZnO thin films on substrate Si (100) at 473 K by using facing target RF magnetron sputtering system at different oxygen pressure and investigated comprehensively the effects of oxygen pressure on the structure, surface morphology and photoluminescence property of ZnO thin films. The results showed that the oxygen pressure play a key role in the structure, surface morphology and photoluminescence property of ZnO thin films and ZnO film deposited at 1.2 Pa Ar pressure and 0.6 Pa oxygen pressure had the best preferential *C*-axis orientation, the weakest compressive stress, the best thin film quality, the strongest ultraviolet (UV) emission and the weakest blue emission, implying that facing target RF magnetron sputtering method is another possible practical applications for the growth of high quality ZnO thin films used in UV apparatus.

Acknowledgements This work was supported by the National Natural Science Foundation of Shandong Province of China (No. 2005ZX11 and No. Y2006A02).

References

1. Özgür Ü, Alivov YI, Liu C, Teke A, Reshchikov MA, Dogan S, Avrutin V, Cho SJ, Morkoc H (2005) J Appl Phys 98:041301
2. Look DC (2001) Mater Sci Eng B 80:383
3. Muthukumar S, Gorla CR, Emanetoglu NW, Liang S, Lu Y (2001) J Cryst Growth 225:197
4. Makino T, Isoya G, Segawa Y, Chia CH, Yasuda T, Kawasaki M, Ohtomo A, Tamura K, Koinuma H (2000) J Cryst Growth 214/215:289
5. Liu M, Wei XQ, Zhang ZG, Sun G, Chen CS, Xue CS, Zhuang HZ, Man BY (2006) Appl Surf Sci 252:4321

6. Znaidi L, Soler-Illia GJAA, Benyahia S, Sanchez C, Kanaev AV (2003) Thin Solid Films 428:257
7. Ondo-Ndong R, Ferblantier G, Kalfioui MA, Boyer A, Foucaran A (2003) J Cryst Growth 255:130
8. Ondo-Ndong R, Dellanoy FP, Boyer A, Giani A, Foucaran A (2003) Mater Sci Eng B 97:68
9. Wang QP, Zhang DH, Xue ZY, Zhang XJ (2004) Opt Mater 26:23
10. Xue ZY, Zhang DH, Wang QP, Wang JH (2002) Appl Surf Sci 195:126
11. Hayashi Y, Kondo K, Murai K, Moriga T, Nakabayashi I, Fukumoto H, Tominaga K (2004) Vacuum 74:607
12. Chen JJ, Gao Y, Zeng F, Li DM, Pan F (2004) Appl Surf Sci 223:318
13. Hong RJ, Qi HJ, Huang JB, He HB, Fan ZX, Shao JD (2005) Thin Solid Films 473:58
14. Cebulla R, Wendt R, Ellmer K (1998) J Appl Phys 83:1087
15. Fang ZB, Gong HX, Liu XQ, Xu DY, Huang CM, Wang YY (2003) Acta Phys Sin 52:1748
16. Xu XL, Guo CX, Qi ZM, Liu HT, Xu J, Shi CS, Chong C, Huang WH, Zhou YJ, Xu CM (2002) Chem Phys Lett 364:57
17. Lin BX, Fu ZX, Jia YB, Liao GH (2001) Acta Phys Sin 50:2208
18. Mahamuni S, Borgohain K, Bendre BS, Leppert VJ, Risbud SH (1999) Appl Phys Lett 85:2861